Turkish Journal of Earth Sciences

http://journals.tubitak.gov.tr/earth/

Research Article

Turkish J Earth Sci
(2013) 22: 1020-1032

doi:10.3906/yer-1204-4

Computation of grade values of sediment-hosted barite deposits in northeastern Isparta (western Turkey)

Numan ELMAS[1,*], **Uğur ŞAHİN**[2]
[1]Regional Directorate of Public Highways, Investigation Department, Hasdal, İstanbul, Turkey
[2]Rochester Institute of Technology, Multi-Agent Bio-Robotics Laboratory, Rochester, NY, United States

Received: 10.04.2012 • **Accepted:** 26.03.2013 • **Published Online:** 11.10.2013 • **Printed:** 08.11.2013

Abstract: Grade value is a crucial parameter for the mineral industry. Investigation of grade value of mineral resources provides the optimum benefit. In this study, an adaptive neuro-fuzzy inference system (ANFIS) and artificial neural network (ANN) model were applied for the prediction of grade values. The spatial coordinates X, Y, and Z of the study area along with bore hole geochemical data were used as input variables in the model. In order to illustrate the applicability and capability of these methods, the western part of Turkey, between the latitudes 38°01′45″N and 38°09′52″N and between the longitudes 31°23′20″E and 31°32′52″E was chosen as the case study area. Measured grades of barite samples were obtained from 47 boreholes using the chemical analysis method. The performance of these models in training and testing sets were evaluated and compared with the observations. The results indicate that the ANFIS model is better than the ANN model and can successfully provide high accuracy and reliability for grade estimation.

Key words: Sedimentary barite, adaptive neuro-fuzzy inference system, artificial neural network, grade estimation, uncertainty, membership function, rule base

1. Introduction

Grade estimation of mineral resources is essential for economic planning in the mineral industry. The grade values are used seriously for production scheduling and mine planning. In practice, the true value of an ore body is never exactly known until it is mined out. Mining investment costs can be decreased using feasible grade estimation methods. Grade estimation contains many uncertainties, which may be due to the sampling, the natural characteristics of an ore deposit, and the analytical error of the chemical and mineralogical analyses (Tütmez 2007). This uncertainty factor in grade estimation leads to the need to develop new estimation methodologies by which financiers and managers can be assisted in evaluating their mining projects with a minimum risk of incorrect prediction (Pham 1997).

Dealing with these uncertainties using different mathematical methods has been discussed in detail (Bardossy & Fodor 2001). A number of methods such as geometrical and geostatistical approaches have been developed for the purpose of grade estimation. Geometrical methods (David 1977) depend on geometrical relationships between sample points, while geostatistical methods (Journel & Huijbregts 1981; Goovaerts 1997) are based on random functions and consider spatial relationship of the sample data used in the analysis (Tütmez 2007). The most important shortcoming of the geostatistical methods is the amount of data. In the case of small deposits, the number of boreholes is not sufficient for the calculation of acceptable variograms. Therefore, geostatistical methods cannot be applied in small deposits. Bardossy and Fodor (2004) have also discussed the advantages and disadvantages of geostatistical methods for reserve estimation and they stressed that geostatistical methods have some limitations. Geostatistical calculation needs suitable computer programs and a considerable mathematical background. Additional limitations of geostatistics were pointed out in detail by Diehl (1997).

On the other hand, the applicability of new mathematical methods in geological estimations has been discussed in detail by Bardossy & Fodor (2001). One of these mathematical methods, fuzzy set and fuzzy modeling theory, which provides new tools for describing uncertain systems using rule bases and new techniques for the inference mechanism, has been applied in reserve estimation (Pham 1997; Tütmez 2007; Tütmez & Dağ 2007). Fuzzy set theory plays an important role in dealing with uncertainty when making decisions in applications

* Correspondence: elmasnuman@yahoo.com

(Dubois & Prade 1998; Kuncheva et al. 1999; Nauck & Kruse 1999). Fuzzy modeling for grade and reserve estimation is a very effective method for mining cost assessments (Pham 1997; Bardossy & Fodor 2001; Tütmez et al. 2007). Integrating geostatistical concepts with fuzzy set theory (Bardossy et al. 1990) is a novel direction, and the application of fuzzy modeling in reserve estimation is very limited. In the literature, Pham (1997) estimated unknown ore grades within a mining deposit in a fuzzy environment using fuzzy c-means clustering and a fuzzy inference system. Galatakis et al. (2002) performed a study for lignite quality estimation using a neural-fuzzy system. The main shortcomings of these works were that the spatial variability of data values could not be used in the algorithms. However, the spatial positions of data directly connected with data values (grades) are very important for reserve estimation (Tütmez 2007). Recently, Luo and Dimitrakopoulos (2003), Bardossy et al. (2003), Bardossy & Fodor (2005), and Tütmez (2005) have applied the fuzzy set theory in resource estimation and mathematically evaluated the spatial continuity of ore bodies by using fuzzy sets. Similarly, Tutmez et al. (2007) carried out a study that tried to combine fuzzy algorithms and spatial variability in reserve estimation.

The other technique emerging as an alternative in recent times is artificial neural network (ANN) models. ANNs have been applied successfully to many problems. Zhang et al. (2007) implemented ANNs for coal mining information fusion. Al Thyabat (2008) used ANN for the optimization of froth flotation. Çilek (2002) investigated the application of back propagation (BP) networks in order to predict the effect of changing flotation variables on the number of cleaning and scavenging stages in a continuous flotation circuit. Nakhhei et al. (2012) investigated metallurgical performance (grade and recovery) forecasting of pilot plant flotation columns by using ANN and multivariate non-linear regression (MNLR) models.

The advantages of both artificial neural networks and fuzzy logic (FL) are combined in the architecture of adaptive neuro-fuzzy inference systems (ANFIS). ANFIS uses a hybrid-learning algorithm to identify parameters of Takagi–Sugeno-type fuzzy inference systems. It applies a combination of the least-squares method and the BP gradient descent method for training membership function (MF) parameters to emulate a given training data set (Soygüder & Alli 2009). Tahmasebi & Hezarkhani (2010, 2012) introduced a new neuro-fuzzy method based on ANN and FL called coactive neuro-fuzzy inference system (CANFIS), which combines the 2 approaches of ANN and FL, and was carried out through a case study in the Sungun copper deposit located in East Azerbaijan, Iran.

The present study investigates the grade estimation of barite mineral based on ANFIS and ANN using spatial coordinates (UTM) along with borehole geochemical input data. The study is the first crucial investigation for barite grade estimation in western Turkey. To identify the relationship between spatial variability and grade value, an ANN and a Takagi–Sugeno type fuzzy model were constructed and the parameters were obtained from data values that describe the system behavior. A systematic data-driven procedure based on spatial variability for grade estimation was developed. A case study was conducted on the prediction of barite grade values in the western Turkey (Isparta) barite deposits. Spatial relationships with the grade value are used in each stage of the model. It is also suitable for grade estimation of any other type of mineral deposits. Mineable and economic reserves can be also calculated by the method suggested here. Finally, the estimation results can serve as a basis for risk calculations of mining investments as well.

2. Depositional characteristics

In the western Turkey (Isparta) barite deposits (Figure 1), barite was mainly deposited in 2 sections: northwestern and southeastern deposits. The northwestern section deposits (Dikmentepe, Ekiztepe, Subaşıpınarı, Cemil Yaşar, and Kızıllıktepe) have not been mined due to the low-grade values of the barite. However, the southeastern section deposits (Kuyucak, Kıpçak, Başkoyak, and Yellice) are being mined. The barite deposits consist of layers, lensoids, and occasional veins, and are associated with carbonate and pelitic host rocks of Cambrian–Ordovician age in the Sultan Mountain metamorphic sequences (Ayhan 1986). The barite grade is above 90% especially in the southeastern part.

2.1. Geological setting

The barite deposits of the study area (Figure 1) occur in Early Paleozoic (Cambrian–Early Ordovician) host rocks (Cortecci *et al.* 1989; Zedef *et al.* 1995; Sharma *et al.* 2006). The stratigraphic units of Early Paleozoic age consist of carbonate and slightly metamorphic rocks. The carbonate rocks (Çaltepe Formation) consist of dolomite and limestones. The slightly metamorphic rocks (Sultandede Formation) are basically divided into 2 units: Seydişehir metamorphics (schist, calc-schist, phyllitic schist, metalimestone, and metasandstone) and Sariyayla limestone (Demirkol 1982; Özgül *et al.* 1991). Thickly layered barites were hosted by the meta-limestone and calc-schist of the Seydişehir metamorphics (Demirkol 1977; Özgül *et al.* 1991). The Mesozoic Hacıalabaz Formation consists of dolomite, limestone, and basic intrusive rocks. It does not include barite mineralization (Öncel 1995). The Miocene Bagkonak Formation comprises terrestrial uncompacted sediments such as gravel, sand, silt, and clay.

2.2. Grade properties

Barite grade properties depend on their geological, geochemical, and structural characteristics. These barite

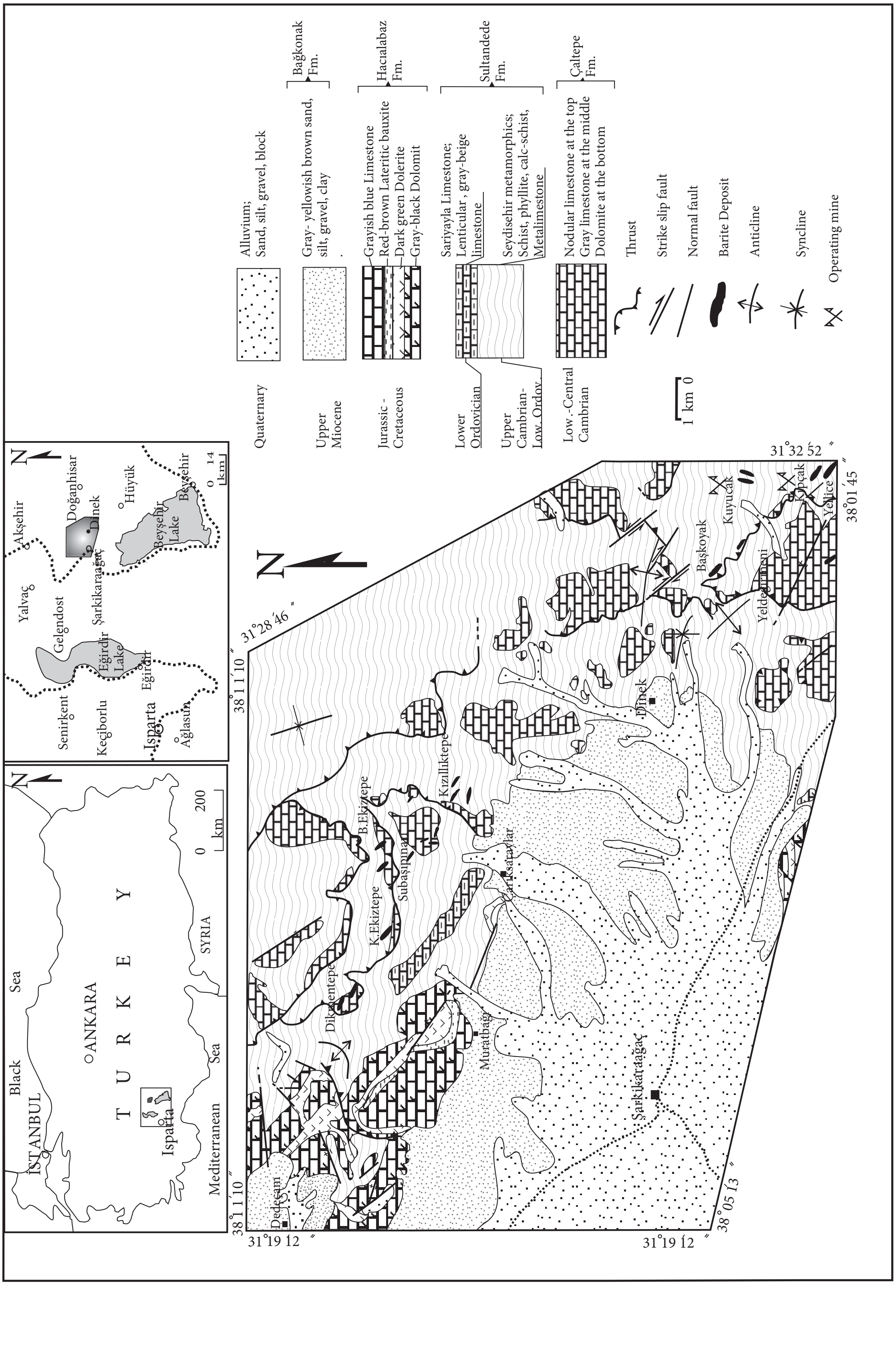

Figure 1. Location and geological map of the study site.

deposits were rotated by NW–SE faults that formed after the mineralization (Koçyiğit 1983). Contaminants can penetrate to the ore body by means of faults, folds, fractures, etc. (Cortecci *et al.* 1989; Maynard & Okita 1991; Arehart 1998; Bozkaya & Gökçe 2004). Thinly layered folded barites and thickly layered fractured, faulted and brecciated barites have low $BaSO_4$ grade values because of ferric oxide contamination (Zimmerman 1969; Ayhan 2001). The amount of gangue minerals (Pb, Zn and Cu-sulfides, Fe-oxides, quartz, Ca-, Cu-, and Fe-carbonates) can also reduce the grade values of barite deposits.

The southeastern barite deposits have higher grade values than the northwestern barites. The highest grade values were estimated in Yellice (97.56%), Başkoyak (95.56%), and Kıpçak (94.65%), while minimum grade values were estimated in the Dikmentepe deposit (76.08%) (Table 1). All of the contaminants cause the reduction of grade and quality of the barite ores. Sulfide contaminations of barite, primarily in the form of galena and to a lesser extent as Cu, Zn, Hg, and As sulfides, are dominantly observed in the northwestern deposits. Therefore, the mine operators abandoned these mines.

3. Methodology

In this study, ANFIS and ANN are used for grade estimation of sediment-hosted barite deposits in the northeastern part of the Isparta ore province, using spatial coordinates X (easting), Y (northing), and Z (height) along with borehole geochemical data from working and abandoned barite mines. This study is the first application for the computation of grade values in western Anatolia. For the grade estimation study, 47 barite samples were collected from the boreholes of the deposits.

3.1. Neuro-fuzzy modeling

Neuro-fuzzy (NF) modeling refers to the method of applying various learning techniques developed in the ANN literature to fuzzy modeling or to a fuzzy inference system (FIS). ANNs are able to learn a kind of process connection from given examples of input–output data. They consist of independent processing units (neurons) and simulate the processing principle of biological networks like the human brain. A high computation rate and a high degree of robustness and failure tolerance are the advantages of ANNs. In addition, they have the ability to generalize and to learn adaptively (Heine 2008).

Fuzzy logic is another method of artificial intelligence. The key idea of fuzzy logic theory is that it allows for something to be partly true, rather than having to be either all true or all false. The degree of "belongingness" to a set or category can be described numerically by a membership number between 0 and 1. The variables are "fuzzified" through the use of a membership function that defines the membership degree to fuzzy sets. These variables are called linguistic variables. Membership functions are curves that define how each point in the input space is mapped to a membership value in the interval {0,1}. It can be of different forms including a triangle, trapezium, or Gauss curve. The fuzzy rule model operates on an "IF–THEN" principle, where the "IF" is a vector of fuzzy explanatory variables of premises (input) and "THEN" is fuzzy consequence or dependent variable (output). Fuzzy logic allows the user to capture uncertainties in data (Chang & Chang 2006).

The basic structure of an FIS consists of 3 conceptual components: a rule base, which contains a selection of fuzzy rules; a database that defines the MFs used in the fuzzy rules; and a reasoning mechanism, which performs the inference procedure upon the rules to derive an output. FIS implements nonlinear mapping from its input space to the output space. This mapping is accomplished by a number of fuzzy if–then rules. The parameters of the if–then rules (antecedents or premises in fuzzy modeling) define a fuzzy region of the input space, and the output parameters (also consequents in fuzzy modeling) specify the corresponding output. Hence, the efficiency of the FIS depends on the estimated parameters. However, the selection of the shape of the fuzzy set (described by the antecedents) corresponding to an input is not guided by any procedure (Mehta & Jain 2009). However, the rule structure of an FIS makes it possible to incorporate human expertise about the system being modeled directly into the modeling process to decide on the relevant inputs, number of MFs for each input, and the corresponding numerical data for parameter estimation. In this study, the concept of the adaptive network, which is a generalization of the common back-propagation neural network, is employed to tackle the parameter identification problem in an FIS. This procedure of developing an FIS using the framework of adaptive neural networks is called an ANFIS (Jang 1993). As the name suggests, ANFIS combines the fuzzy qualitative approach with the neural network adaptive capabilities to achieve a desired performance (Chang & Chang, 2006). The details of adaptive networks have been described by researchers (Jang 1993) and a novel architecture and learning procedure for the FIS that uses a neural network learning algorithm for constructing a set of fuzzy if–then rules with appropriate MFs from the stipulated input–output pairs has been introduced (Jang 1993; Jang & Sun 1995; Mehta & Jain 2009). In this study, the well-known adaptive algorithm called ANFIS is used with the aid of the Matlab Fuzzy Logic Toolbox.

3.2. Model architecture

1. ANN model: ANNs are computing systems made up of a large number of firmly interconnected adaptive processing elements (neurons) that are able to perform massively parallel computations for data processing and knowledge representation. Learning in ANNs is accomplished

Table 1. Chemical compositions of the barite samples.

Region -sample	*$BaSO_4$*	*BaO*	*CaO*	*MgO*	*SrO*	*SiO_2*	*Al_2O_3*	*Fe_2O_3*	*ZnO*	*PbO*	*Cu*	*Cd*	*As*	*Sb*	*Bi*	*Mo*
no	%	%	%	%	%	%	%	%	%	%	ppm	ppm	ppm	ppm	ppm	ppm
DT01	76.08	49.98	2.32	0.80	2.3	3.75	0.10	0.38	0.8	9.2	600	300	250	100	45	45
DT21	76.45	50.22	0.75	0.81	2.6	0.79	0.14	0.51	0.9	9.0	610	100	240	95	45	45
DT22	77.25	50.25	1.21	0.92	2.4	2.37	0.17	0.84	1.0	7.8	590	90	250	95	40	40
DT41	78.81	51.77	0.83	0.95	4.2	0.87	0.11	0.85	1.1	7.8	595	95	240	100	40	40
DT45	78.88	51.82	0.35	0.85	3.1	1.62	0.10	0.80	1.0	8.1	600	110	260	95	45	45
DT07	80.87	53.13	1.25	0.83	2.3	1.60	0.10	0.75	1.0	9.1	610	110	260	100	50	40
DT17	80.56	52.92	0.25	0.86	3.2	0.83	0.15	0.85	1.1	6.2	590	95	260	95	45	35
DT23	75.92	50.05	0.75	0.89	3.5	0.95	0.20	0.87	1.2	6.4	620	96	258	98	50	35
DT33	79.12	51.80	0.30	0.85	3.4	0.80	0.20	0.84	1.0	6.1	600	100	250	95	45	40
BE03	87.55	57.52	2.91	0.55	2.1	0.57	0.21	0.70	0.6	2.0	550	80	175	85	95	60
BE11	88.68	58.26	3.93	0.57	4.0	0.45	0.16	0.70	0.6	2.0	550	75	185	85	95	60
BE21	89.25	58.63	2.07	0.63	2.8	0.53	0.28	0.30	0.6	2.0	500	85	180	87	95	65
BE03	90.15	59.22	1.05	0.54	2.8	0.48	0.31	0.60	0.5	1.9	575	90	175	87	90	65
KE14	90.38	59.37	0.85	0.45	3.2	0.67	0.24	0.60	0.5	1.9	550	70	170	82	90	70
KE16	91.32	59.99	1.33	0.58	2.7	0.85	0.11	0.70	0.6	1.8	575	75	170	82	95	65
KE23	90.75	59.62	1.45	0.45	3.4	1.13	0.12	0.70	0.6	2.0	575	85	165	86	95	60
KE04	91.85	60.34	1.02	0.52	3.3	1.32	0.10	0.60	0.7	2.1	500	90	190	87	85	60
SP01	83.38	54.78	0.74	0.94	4.2	2.05	0.26	0.80	0.7	4.5	700	75	190	120	115	90
SP12	84.37	55.43	0.82	0.91	4.1	2.35	0.20	0.80	0.7	4.5	710	70	190	110	110	95
SP22	88.12	57.93	0.95	1.08	4.6	2.69	0.27	0.81	0.6	5.6	700	72	195	120	120	90
SP33	83.80	61.21	0.88	0.90	4.2	2.36	0.24	0.80	0.7	4.8	720	70	190	125	115	95
CY01	85.86	56.41	2.85	0.95	4.3	0.75	0.07	0.70	0.7	3.6	720	70	195	110	110	95
CY02	86.82	57.04	1.96	0.97	4.5	3.18	0.08	0.70	0.6	4.5	720	68	185	120	110	90
CY03	84.70	60.35	2.15	0.95	4.6	2.88	0.09	0.75	0.7	4.5	730	70	185	120	115	95
CY13	87.67	57.59	1.18	0.95	4.3	1.28	0.10	0.80	0.7	4.5	710	72	185	125	115	85
KT01	89.69	58.92	0.78	0.85	4.7	2.12	0.15	0.85	0.8	4.6	700	74	190	125	115	80
KT21	88.18	57.93	0.55	0.90	4.1	0.86	0.12	0.85	0.8	4.5	710	68	180	120	115	95
KT 31	88.36	58.25	0.70	0.85	4.5	1.95	0.18	0.82	0.8	4.2	700	75	195	125	115	90
KT 41	88.45	58.30	0.75	0.85	4.5	1.90	0.20	0.85	0.8	4.2	700	73	190	125	120	85
KT 51	87.65	57.95	1.00	0.90	4.0	1.90	0.25	0.85	0.9	4.1	720	75	190	125	120	85
Y011	97.15	63.82	2.83	0.05	0.8	0.25	0.18	0.80	0.4	0.2	400	25	100	65	80	45
Y025	96.47	63.38	1.82	0.08	1.2	0.08	0.68	0.70	0.5	0.5	450	45	120	75	70	40
Y030	96.80	63.42	1.80	0.08	1.1	0.08	0.70	0.70	0.5	0.5	450	45	120	75	70	40
Y035	95.92	62.15	1.00	0.06	1.2	0.09	0.70	0.70	0.5	0.5	450	45	120	75	70	40
Y012	97.56	63.88	2.01	0.05	1.0	0.09	0.75	0.70	0.5	0.5	450	45	120	75	70	40
B001	95.56	62.78	0.71	0.04	1.6	0.93	0.05	0.90	0.3	0.4	400	36	110	70	70	45
B002	94.80	62.20	0.75	0.05	1.5	0.95	0.05	0.95	0.4	0.4	450	38	115	70	70	45
B003	94.72	62.18	0.75	0.05	1.6	0.95	0.05	0.95	0.4	0.4	450	40	110	75	70	45
KP02	94.65	62.18	0.83	0.02	1.4	0.85	0.07	0.95	0.3	0.5	375	37	95	60	85	45
KP22	94.58	62.13	0.97	0.03	1.0	0.25	0.09	0.75	0.5	0.5	390	15	95	65	65	35
KP25	94.26	61.85	0.95	0.04	1.2	0.32	0.08	0.75	0.5	0.5	420	15	95	60	70	40
KP30	95.52	62.58	0.65	0.04	1.5	0.65	0.09	0.80	0.6	0.5	450	25	90	55	75	45
KU12	92.76	60.94	1.02	0.08	1.1	3.32	0.31	0.82	0.3	0.2	350	28	100	60	90	38
KU14	91.48	60.10	0.63	0.03	0.8	3.63	0.64	0.75	0.3	0.4	400	35	110	65	90	45
KU25	90.08	59.18	0.99	0.03	1.4	2.05	0.69	0.75	0.4	0.6	425	40	115	65	85	45
KU27	94.15	61.75	0.95	0.05	1.3	1.80	0.59	0.70	0.3	0.6	400	40	110	60	85	45
KU31	93.28	60.85	0.95	0.05	1.4	1.65	0.50	0.80	0.4	0.8	450	40	115	65	85	45

through special training algorithms developed based on learning rules presumed to mimic the learning mechanisms of biological systems. ANNs can be trained to recognize patterns and the nonlinear models developed during training allow neural networks to generalize their conclusions and to make applications to patterns not previously encountered (Haykin 1994; Chaudhuri & Bhattacharya 2000).

A multilayer perceptron (MLP) has features such as the ability to learn and generalize, smaller training set requirements, fast operation, and ease of implementation, which make it the most commonly used neural network architecture. Currently, the most widely used ANN type is a MLP that has been playing a central role in the application of neural networks. The MLP is a nonparametric technique for performing a wide variety of detection and estimation tasks. In the MLP, each neuron *j* in the hidden layer sums its input signals x_i after multiplying them by the strengths of the respective connection weight w_{ji} and computes its output y_j as a function of the sum

$$y_j = f(\Sigma w_{ji} x_i) \tag{1}$$

where *f* is the activation function that is essential to transform the weighted sum of all signals mapping onto a neuron. The activation function (*f*) can be a simple threshold function, or a sigmoid, hyperbolic tangent, or radial basis function. The sum of the squared differences between the desired and actual values of the output neurons *E* is defined as

$$E = \frac{1}{2}\sum_j (y_{dj} - y_j)^2 \tag{2}$$

where y_{dj} is the desired value of output neuron *j* and y_j is the actual output of that neuron. Each weight w_{ji} is adjusted to reduce *E* as rapidly as possible. How w_{ji} is adjusted depends on the training algorithm adopted (Basheer & Hajmeer 2000; Guler & Ubeyli 2005; Zhihong & Zhizeng 2008).

Usually, a network consists of 1 input layer, 1 output layer, and 1 or 2 hidden layers. Each connection is associated with a connection weight. During the learning phase, the network is presented with a set of known input and output values called patterns. Using an optimal learning algorithm (a gradient descent back-propagation algorithm for this study), the weights are modified iteratively, and after a number of iterations they get adjusted in such a way that when the input values are presented, the network produces outputs that are close to their actual output values.

2. ANFIS model: To present the ANFIS architecture, let us consider 2 fuzzy rules based on a first order Sugeno model:

$$Rule1: if\ (x\ is\ A_1)\ and\ (y\ is\ B_1)\ then\ f_1 = p_1 x + q_1 y + r_1$$

$$Rule2: if\ (x\ is\ A_2)\ and\ (y\ is\ B_2)\ then\ f_2 = p_2 x + q_2 y + r_2$$

The ANFIS architecture to implement these 2 rules is shown in Figure 2. Note that a circle indicates a fixed node whereas a square indicates an adaptive node (the parameters are changed during adaptation or training). In the following presentation, O_{li} denotes the output of node *i* in layer 1.

Layer 1: All the nodes in this layer are adaptive nodes. The output of each node *i* is the degree of membership of the input to the fuzzy MF represented by the node:

$$O_{1,i} = \mu_{Ai}(x), i = 1,2$$

$$O_{1,i} = \mu_{Bi-2}(x), i = 3,4$$

A_i and B_i can be any appropriate fuzzy sets in parameter form. For example, if the Gauss MF is used, then

$$\mu_{Ai}(x) = e^{-(\frac{x-c_i}{a_i})^2}$$

where a_i and c_i are the parameters for the MF.

Layer 2: The nodes in this layer are fixed (not adaptive). They are labeled M to indicate that they play the role of a simple multiplier. The outputs of these nodes are given by:

$$O_{2,i} = w_i = \mu_{Ai}(x)\mu_{Bi}(x) \qquad \boldsymbol{i} = 1,2,$$

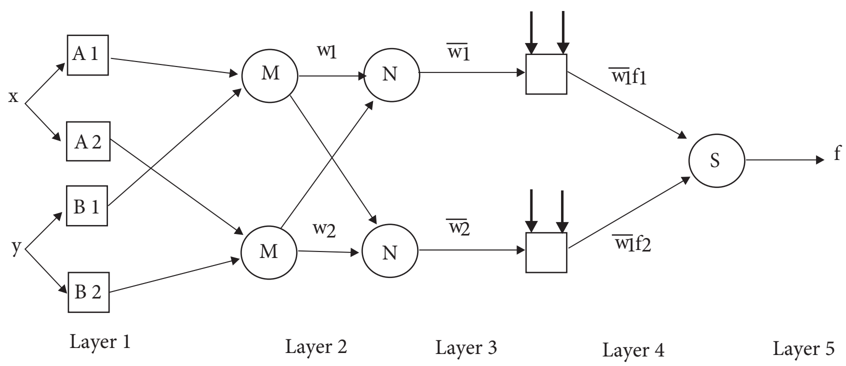

Figure 2. ANFIS architecture. A circle indicates a fixed node whereas a square indicates an adaptive node (the parameters are changed during adaptation or training).

The output of each node in this layer represents the firing strength of the rule.

Layer 3: Nodes in this layer are also fixed nodes. They are labeled N to indicate that they perform a normalization of the firing strength from the previous layer. The output of each node is given by:

$$O_{3,i} = \overline{w} = \frac{w_1}{w_1 + w_2} \qquad \boldsymbol{i} = 1,2,$$

Layer 4: All the nodes in this layer are adaptive nodes. The output of each node in this layer is simply the product of the normalized firing strength and a first order polynomial (for a first order Sugeno model):

$$O_{4,i} = \overline{w}_i f_i = \overline{w}_i (p_i x + q_i y + r) \quad \boldsymbol{i} = 1,2,$$

where p_i, q_i, and r_i are design parameters (referred to as consequent parameters since they deal with the "then" part of the fuzzy rule).

Layer 5: This layer has only 1 node labeled S to indicate that it performs a simple summing function. The output of this single node is given by:

$$O_{5,i} = \sum_i \overline{w}_i f_i = \frac{\sum_i w_i f_i}{\sum_i w_i} \qquad \boldsymbol{i}=1,2,$$

The ANFIS architecture is not unique. Some layers can be combined and still produce the same output. In this ANFIS architecture, there are 2 adaptive layers (layers 1 and 4). Layer 1 has 2 modifiable parameters (a_i and c_i) pertaining to the input MFs. These parameters are called premise parameters. Layer 4 also has 3 modifiable parameters (p_i, q_i and r_i) pertaining to the first order polynomial. As mentioned earlier, these parameters are called consequent parameters. The task of the training or learning algorithm for this architecture is to tune all the modifiable parameters to make the ANFIS output match the training data. If these parameters are fixed, the output of the network becomes:

$$f = \frac{w_1}{w_1 + w_2} \mathrm{f}_1 + \frac{w_1}{w_1 + w_2} f_2 =$$
$$\overline{w}_1 f_1 + \overline{w}_2 f_2 = \overline{w}_1 (p_1 x + q_1 y + r)\, \overline{w}_1 (p_2 x + q_2 y + r)$$
$$= (\overline{w}_1 x) p_1 + (\overline{w}_1 y) q_1 + (\overline{w}_1) r_1 +$$
$$(\overline{w}_2 x) p_2 + (\overline{w}_2 y) q_2 + (\overline{w}_2) r_2$$

which is a linear combination of the modifiable parameters. Therefore, a combination of gradient descent and the least-squares method can easily identify the optimal values for the parameters p_i, q_i and r_i. However, if the MFs are not fixed and are allowed to vary, then the search space becomes larger and, consequently, the convergence of the training algorithm becomes slower (Jang 1992). A hybrid algorithm combining the least-squares method and the gradient descent method was adopted to solve this problem. The hybrid algorithm is composed of a forward pass and a backward pass. The least-squares method (forward pass) is used to optimize the consequent parameters with the premise parameters fixed. Once the optimal consequent parameters are found, the backward pass starts immediately. The gradient descent method (backward pass) is used to optimally adjust the premise parameters corresponding to the fuzzy sets in the input domain. The output of the ANFIS is calculated by employing the consequent parameters found in the forward pass. The output error is used to adapt the premise parameters by means of a standard back-propagation algorithm. It has been proven that this hybrid algorithm is highly efficient in training the ANFIS (Jang 1993; Jang & Sun 1995). Therefore, in this study, the proposed ANFIS model was trained with the back-propagation gradient descent method in combination with the least-squares method.

4. Results and discussion

4.1. Application for barite grade estimation

For grade estimation using a neural network, 3D spatial coordinates were used as input variables, and grade attribute was used as an output variable for the respective data sets. The complex spatial structure between input and output patterns is captured through a network via a set of connection weights that are adjusted during the training of the networks. The network captures an input–output relationship through training and acquires a certain prediction capability so that for a given input the network produces an output (grade).

The network consisted of an input layer containing 3 input nodes (for the 3 spatial coordinates), an output layer consisting of an output node corresponding to grade attribute, and a hidden layer composed of 11 nodes. Logistic activation was used in both the hidden and output nodes. It can be noted that while the numbers of input and output nodes for a given problem are fixed, the user has the flexibility to change the number of hidden nodes according to the neural network performance. After trial and error testing, 11 hidden nodes were chosen, which resulted in the minimum average error rates in the testing set.

The best network geometry was chosen according to the highest correlation and the lowest root mean square error (RMSE). When the training was completed, the network was tested for its learning and generalization capabilities. The test for generalization ability was carried out by investigating its capability to predict the output sets that were not included in the training process. For this purpose, about 7 new data had been selected. The results of the agreement between the measured and predicted values of the output nodes and the prediction error values are shown in Figure 3. The proposed model demonstrated the ability of a feed-forward BP neural network to predict the grade value with sufficient accuracy. The model performed quite well in predicting not only the efficiency of the treatment of the data used in the training process, but also that of test data that were unfamiliar to the neural network.

For the fuzzy model, various NF model architectures were tried and the appropriate model structure was determined by comparing them all using the same statistical parameters, which are given in Table 2. It is possible to estimate the grade from the spatial variables X, Y, and Z. The spatial coordinates were normalized to a 0–1 interval.

For each input variable, gaussian-type MFs were used and the range of the inputs was divided into the 6 fuzzy subsets VL = very low, L = low, M = medium, FM = fairly medium, H = high, and VH = very high, after trying other alternatives for the MF number (Figure 3).

In the parameter estimation process performed by ANFIS, the 47 data values recorded in different sections of the region (Figure 4) were divided into 3 independent subsets: training, verification or checking, and testing. The training subset included 29 data points, the verification subset had 11, and the testing subset had the remaining 7. First, the training subsets were repeatedly used to build a NF model and to adjust the connected weights of the constructed networks. Afterward, the verification subset was used to simulate the performance of the built models to check their suitability for generalization, and the best fuzzy model was selected for further use. The testing data values were then used for final evaluation of the selected network performance. It is worth mentioning that the testing values must be unseen by the model in the training and verification phases. All data values were selected randomly. Statistically, 47 data values are enough to deduce scientifically significant conclusions but the number of data depends on the event and the model used as well. For instance, the greater the serial correlation, the lower is the amount of data needed in any model study. On the other hand, in some investigations the data cannot be obtained easily or economically, which does not mean that the model cannot be constructed. This last statement is particularly valid for ANN and FL modeling. In the ANN approach, the system is trained in such a manner that the available data are digested by the system weightings with a minimum total square error. In FL modeling, the number of data points required can be even smaller because the spread of odd data domain is covered by membership functions (Figure 5).

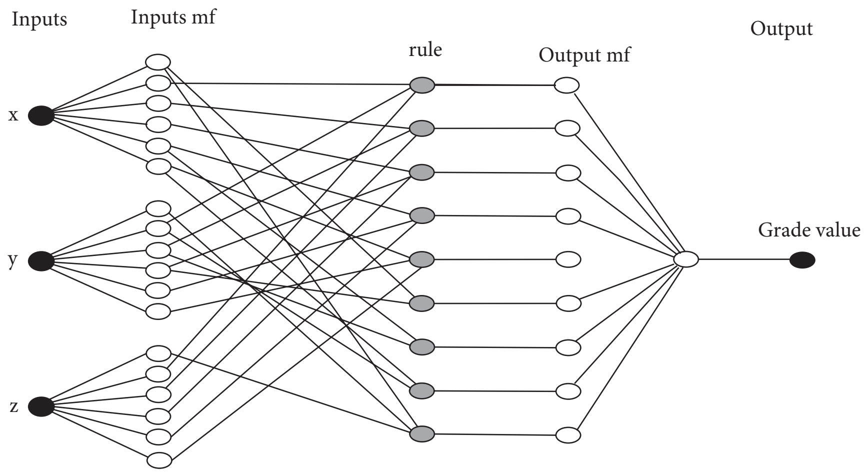

Figure 3. The structure of an ANFIS model for grade value, trained for 200 epochs.

Table 2. Evaluation of the ANFIS and ANN model performances.

	ANFIS		ANN	
	Training data	Testing data	Training data	Testing data
CC	0.97	0.95	0.94	0.92
VAF	0.93	0.89	0.87	0.84
RMSE	1.07	2.17	2.18	2.71

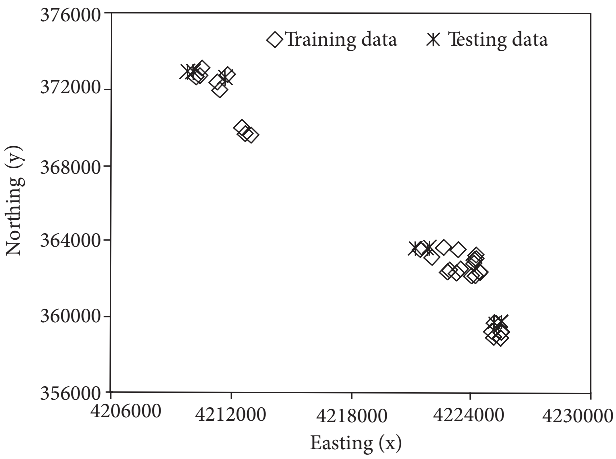

Figure 4. The parameter estimation process performed by ANFIS. The 47 data values recorded in different sections of the region are divided into training, verification or checking, and testing subsets.

Additionally, linguistic information can also be used in the rule base, which reduces the level of the data requirement. Although in general there is a disadvantage to using a limited database, it is less problematic in ANN and especially FL modeling where the rule base covers many deficiencies of the database. The MFs for input variables are shown in Figure 5, and the rules related to the proposed model can be given as follows in the rule base.

4.2. Rule base

The result estimations from the ANN and ANFIS models for the measured data samples are compared in Table 3. The first 6 rules were obtained by applying the ANFIS procedure. The formed ANFIS model was trained for 200 epochs and the structure of the ANFIS model is presented in Table 4. However, the NF model gave unacceptable values for the Quaternary and Mesozoic regions. Therefore, the last 3 rules were added for this region by using expert knowledge.

To obtain an objective perspective of the performance of both models, RMSE, correlation coefficients (CC), and variance accounted for (VAF) statistics were used as evaluation criteria.

The ANFIS and ANN models were compared according to performance and the results are summarized in Table 2. It appears that the ANFIS models are accurate and consistent in different data subsets, where all the values of the RMSE are smaller than the ANN values, all CCs are also very close to unity, and the VAF value is higher than the ANN value. These results might also suggest that the ANFIS has a greater ability to learn from the input–output patterns, which show the coordinates are lumped effects on grade estimation, than the ANN ones.

Figures 6a and 6b show the success of matching the measured and estimated grade values computed with the ANFIS and ANN models in terms of a scatter diagram with respect to combined training–validation data sets and testing phases, respectively. The figures nicely demonstrate that the NF model performance is generally accurate, as all data points roughly fall onto the line of agreement. As seen from the fit line equations and scatter plots in Figure 6 (the equation is in the form of y = a0x + a1), the a0 and a1 coefficients for the NF model are, respectively, closer to 1 and 0 with the determination coefficient (R^2) value of 0.9418 for the training–validation samples and 0.908 for the testing samples. The spatial variation of the observed grade value of the barite deposit and the estimates by using the fuzzy techniques for all the samples are plotted in Figure 6. It can be seen from these graphs that the fuzzy estimates follow the observed values very closely. Figure 7 shows both ANFIS and ANN performance for the measured values. In addition, the 3D variogram of the ANFIS model suggests that grade estimation values of the barite samples are consistent with the measured values (Figure 8). The 3D variogram also indicates the consistency of the grade estimation model with depositional characteristics and grade values of barite.

5. Conclusions

This paper has shown how a neuro-fuzzy and artificial neural network system can be developed to model ore

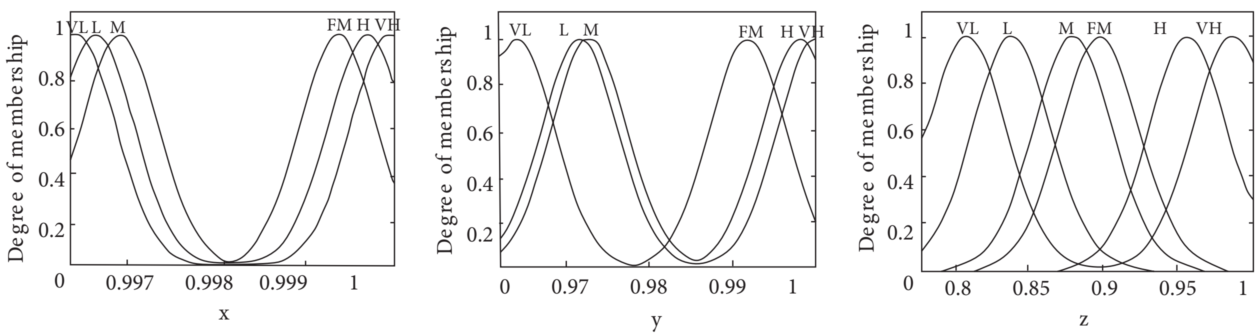

Figure 5. The MFs for input variables and the rules related to the proposed model.

Table 3. Comparison of both models' performances.

Sample	X (Easting)	Y (Northing)	Z (Height)	Grade	ANFIS	ANN
DT23	0.99991	0.96428	0.95808	75.97	78.09	77.56
DT01	1.00000	0.96226	0.95808	76.08	78.07	78.09
DT41	0.99991	0.96300	0.92814	78.81	77.41	80.91
DT33	0.99994	0.96410	0.95808	79.12	78.09	77.62
DT07	0.99995	0.96302	0.98204	80.87	79.16	79.17
SP12	0.99948	0.97278	0.81437	84.37	86.86	87.21
CY03	0.99937	0.97162	0.77844	84.70	85.23	86.96
CY02	0.99940	0.97183	0.83234	86.82	87.54	88.66
2. BE03	0.99970	0.97332	0.89222	87.55	89.53	93.46
CY13	0.99937	0.97166	0.80838	87.67	86.15	88.58
SP22	0.99949	0.97299	0.82036	88.12	87.20	87.30
KT 21	0.99918	0.97347	0.80838	88.18	87.04	88.97
KT 31	0.99932	0.97504	0.86826	88.36	87.91	89.49
BE11	0.99970	0.97392	0.86826	88.68	88.98	91.84
KU25	0.99667	0.99745	0.92814	90.08	89.72	91.64
BE03	0.99962	0.97299	0.89820	90.15	89.74	92.40
KE23	0.99970	0.97282	0.88024	90.75	90.02	92.91
KE16	0.99967	0.97104	0.89820	91.32	91.34	93.33
KU14	0.99665	0.99820	0.89820	91.48	91.59	89.65
KE04	0.99973	0.97166	0.89222	91.85	91.02	94.51
KU27	0.99675	0.99946	1.00000	94.15	94.49	93.13
KP25	0.99642	0.99941	0.94611	94.26	94.85	93.80
KP02	0.99639	1.00000	0.99401	94.65	95.01	94.47
B003	0.99704	0.99098	0.86826	94.72	94.72	94.53
B002	0.99692	0.99196	0.83832	94.80	94.80	94.72
KP30	0.99645	1.00013	0.98802	95.52	95.62	95.88
Y025	0.99640	0.99973	0.97605	96.47	96.81	96.36
Y030	0.99640	0.99962	0.98204	96.80	96.28	96.08
Y012	0.99643	0.99944	0.97904	97.56	96.59	96.22
DT21	0.99995	0.96312	0.95808	76.45	78.08	77.92
DT45	0.99992	0.96243	0.97605	78.88	78.89	79.20
DT17	0.99995	0.96308	0.97605	80.56	78.89	78.67
SP33	0.99950	0.97466	0.83832	83.80	88.23	87.07
CY01	0.99946	0.97162	0.83832	85.86	88.16	88.86
KT 41	0.99905	0.97461	0.79641	88.45	87.30	88.83
BE21	0.99966	0.97254	0.89820	89.25	90.13	93.03
KE14	0.99970	0.97097	0.86826	90.38	91.51	93.54
KU12	0.99665	0.99836	0.95808	92.76	96.92	95.05
KP22	0.99637	0.99949	0.96407	94.58	97.53	95.77
B001	0.99698	0.99123	0.86826	95.56	94.77	93.85
DT22	0.99997	0.96426	0.98802	77.25	79.44	79.80
SP01	0.99949	0.97332	0.80838	83.38	86.88	86.60
KT 51	0.99901	0.97445	0.77844	87.65	86.75	88.44
KT 01	0.99912	0.97461	0.83832	89.69	88.32	90.78
KU31	0.99673	0.99906	0.98802	93.28	95.78	95.48
Y035	0.99632	0.99981	1.00599	95.92	93.75	89.17
Y011	0.99637	0.99995	0.98802	97.15	95.64	95.55

Table 4. ANFIS model structure for the grade estimation (Gauss 2mf-6).

ANFIS parameters	Values
Number of nodes	54
Number of linear parameters	24
Number of nonlinear parameters	36
Total number of parameters	60
Number of training data pairs	29
Number of fuzzy rules	9

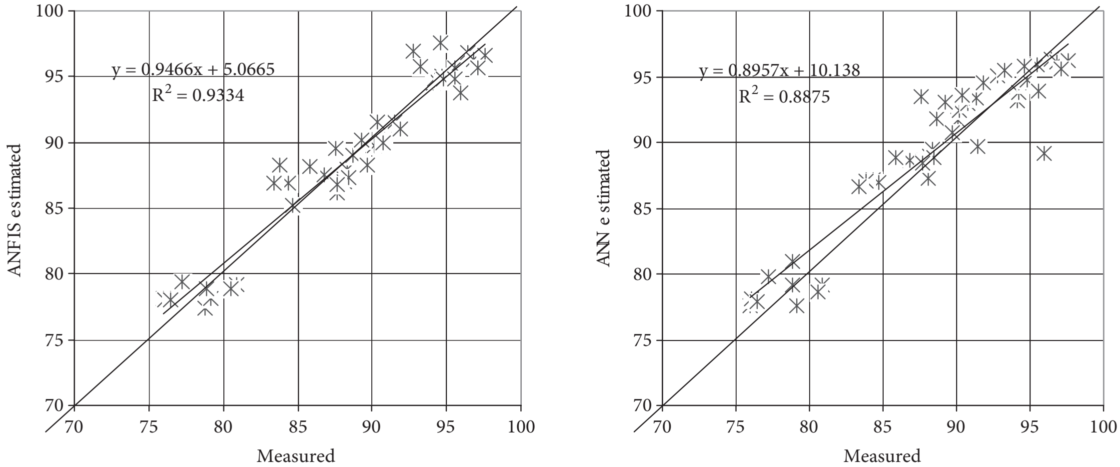

Figure 6. Comparison of the ANFIS and the ANN model estimations in the form of a scatter diagram.

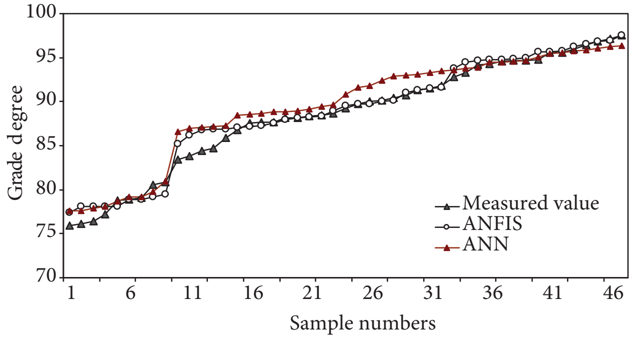

Figure 7. ANFIS and ANN performance for measured grade values.

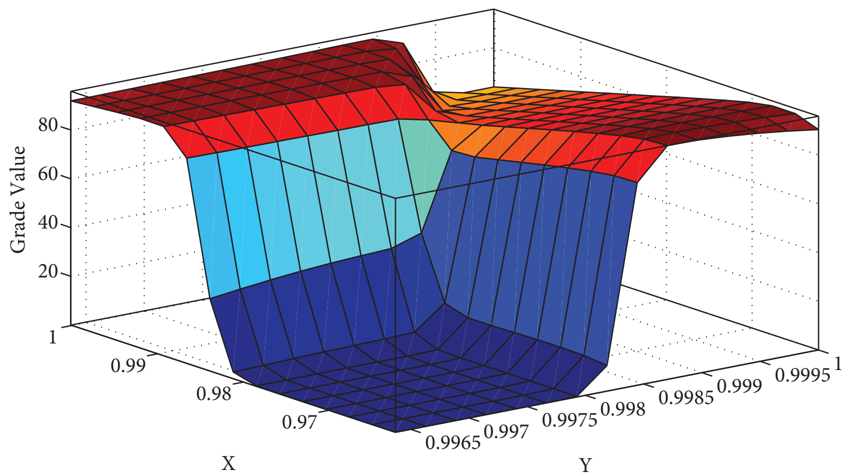

Figure 8. 3D variogram of the ANFIS model. Grade estimation values of the barite samples are consistent with measured values.

grade spatial variability and then be used to estimate ore grades in unknown locations.

The system's architecture was explained and its main components were analyzed. The results obtained from the system have shown clearly the potential of both approaches, even in the case of such a complex deposit as the barite ores used in this paper. Also, it can be seen that the ANFIS application was more successful than the ANN model tested by both simulated and measured data.

The ANFIS method can be efficiently used for tenor estimation of deposits having tabular bodies or bodies that do not show significant thickness and content variation. It should also be noted that the system was developed without performing any statistical analysis on the dataset and without using any information on its geological background, which shows some of the advantages over geostatistics.

References

Al Thyabat, S. 2008. On the optimization of froth flotation by the use of an artificial neural network. *Journal of the China University of Mining and Technology* **18**, 418–426.

Arehart, G.B. 1998. Isotopic signature of hydrothermal sulfates from Carlin-type ore deposits. *In:* Arehart, G.B. & Hulston, J.R. (eds), *Proceedings of the 9th International Symposium on Water-Rock Interaction,* Balkema, 517–520.

Ayhan, A. 1986. The properties of barite occurences in the Lower–Middle Cambrian sedimentary sequences around Huyuk (Konya). *Selçuk University Engineering Faculty Bulletin* **1,** 20–45.

Ayhan, A. 2001. Stratiform barite, deposits between Şarkikaraağaç (Isparta) and Hüyük (Konya) in Sultandağ Section, Turkey. *Chemie der Erde* **61**, 54–66.

Bardossy, G. & Fodor, J. 2001. Traditional and new ways to handle uncertainty in geology. *Natural Resources Research* **10**, 169–187.

Bardossy, G. & Fodor, J. 2004. *Evaluation of Uncertainties and Risks in Geology*. Springer, Heidelberg.

Bardossy, G. & Fodor, J. 2005. Assessment of the completeness of mineral exploration by the application of fuzzy arithmetic and prior information. *Acta Polytechnica Hungarica* **2**, 1–17.

Bardossy, G., Bogardy, I. & Kelly, W.E. 1990. Kriging with imprecise (fuzzy) variograms. II: application: *Mathematical Geology* **22**, 81–94.

Bardossy, G., Szabo, I.R. & Varga, G. 2003. A new method of resource estimation for bauxite and other solid mineral deposits. *Journal of Hungarian Geomathematics* **1**, 14–26.

Basheer, I.A. & Hajmeer, M. 2000. Artificial neural networks: fundamentals, computing, design, and application. *Journal of Microbiological Methods* **43**, 3–31.

Bozkaya, G. & Gökçe, A. 2004. Trace and rare earth element geochemistry of the Karalar (Gazipaşa-Antalya) barite–galena deposits, southeastern Turkey. *Turkish Journal of Earth Sciences* **13**, 63–76.

Chang, F.J. & Chang, Y.T. 2006. Adaptive neuro-fuzzy inference system for prediction of water level in reservoir. *Advances in Water Resources* **29**, 1–10.

Chang, G., Fontes, J.C., Maiorani, A., Perna, G., Pintus, E. & Turi, B. 1989. Oxygen, sulfur and strontium isotope and fluid inclusion studies of barite deposits from the Iglesiente-Sulcis mining district, SW Sardinia Italy. *Mineralium Deposita* **24**, 34–42.

Chaudhuri, B.B. & Bhattacharya, U. 2000. Efficient training and improved performance of multilayer perceptron in pattern classification. *Neurocomputing* **34**, 11–27.

Çilek, E.C. 2002. Application of neural networks to predict locked cycle flotation test results. *Minerals Engineering* **15**, 1095–1104.

David, M. 1977. *Geostatistical Ore Reserve Estimation*. Elsevier, Amsterdam.

Demirkol, C. 1977. *The geology around Yalvaç-Akşehir.* PhD Thesis, Selçuk University, Konya–Turkey [unpublished].

Demirkol, C. 1982. The stratigraphy around Yalvac-Aksehir and its correlation with Western Taurus. *The Bulletin of Engineering Geology* **14**, 3–14.

Diehl, P. 1997. Quantification of the term geological assurance in coal classification using geostatistical methods. *Schriftenreihe der Gesellschaft Deutscher Metallhuetten und Bergleute* **79**, 187–203.

Dubois, D. & Prade, H. 1998. An introduction to fuzzy systems. *Clinica Chimica Acta* **270**, 3–9.

Galatakis, M., Theodoridis, K. & Kouridou, O. 2002. Lignite quality estimation using ANN and adaptive neuro-fuzzy inference systems (ANFIS). *Application of Computers and Mathematics in the Mineral Industries.* 425–431.

Goovaerts, P. 1997. *Geostatistics for Natural Resources Evaluation*. Oxford University Press, New York.

Güler, I. & Ubeyli, E.D. 2005. A mixture of experts network structure for modelling Doppler ultrasound blood flow signals. *Computers in Biology and Medicine* **35**, 565–582.

Haykin, S. 1994. *Neural Networks: A Comprehensive Foundation*. Macmillan, New York.

Heine, K. 2008. Fuzzy technology and ANN for analysis of deformation processes. *In: Proceedings of First Workshop on Application of Artificial Intelligence in Engineering Geodesy,* Vienna, 9–25.

Jang, C. & Jang, J.S.R. 1992. Self-learning fuzzy controllers based on temporal backpropagation. *IEEE Transactions on Neural Networks* **3**, 714–723.

Jang, J.S.R. 1993. ANFIS: Adaptive-network-based fuzzy inference system. *IEEE Transactions on Systems, Man, and Cybernetics* **23**, 665–685.

Jang, J.S.R. & Sun, C.T. 1995. Neuro-fuzzy modeling and control. *Proceedings of the IEEE* **83**, 378–406.

Journel, A.G. & Huijbregts, C.J. 1981. *Mining Geostatistics*. Academic Press, London.

Koçyiğit, A. 1983. The tectonics of Hoyran Lake (Isparta). *Bulletin of the Geological Society of Turkey* **26**, 1–10 [in Turkish with English abstract].

Kuncheva, L.I. & Steinman, F. 1999. Fuzzy diagnosis. *Artificial Intelligence in Medicine* **16,** 121–128.

Li, J., Wang, H., Nienman, D. & Tanaka, K. 2000. Dynamic parallel distributed compensation for Takagi–Sugeno fuzzy systems: an LMI approach. *Information Sciences* **123**, 201–221.

Luo, X. & Dimitrakopoulos, R. 2003. Data-driven fuzzy analysis in quantitative mineral resource assessment. *Computers and Geosciences* **29**, 3–13.

Maynard, J.B. & Okita, P.M. 1991. Bedded barite deposits of the US, Canada, Germany, and China: two major types based on tectonic setting. *Economic Geology* **86**, 364–367.

Metha, R. & Jain, S.K. 2009. Optimal operation of a multi-purpose reservoir using neuro-fuzzy technique. *Journal of Water Resources Management* **23**, 509–529.

Nauck, D. & Kruse, R. 1999. Obtaining interpretable fuzzy classification rules from medical data. *Artificial Intelligence in Medicine* **16**, 149–169.

Öncel, S. 1995. *The Geology of Şarkikaraağaç and Yalvaç (Isparta) and the Mineralogical–Perographical–Geochemical Investigation of Bauxite Occurrences.* PhD Thesis, Selçuk University Institute of Natural Sciences, Konya–Turkey [unpublished].

Özgül, N., Bölükbaşi, S., Alkan, H., Öztaş, Y. & Korucu, M., 1991. Tectono stratigraphic unities in the Lakes regions, *Ozan Sungurlu Symposium*, METU–Ankara, 213–237 [in Turkish].

Pham, T.D. 1997. Grade estimation using fuzzy-set algorithms. *Mathematical Geology* **29**, 291–305.

Sharma, R., Verma, P. & Law, R.W. 2006. Sulphur isotopic study on barite mineralization of the Tons valley, Lesser Himalaya, India: implication for source and formation process. *Current Science* **90**, 440–443.

Soygüder, S. & Alli, H. 2009. An expert system for the humidity and temperature control in HVAC systems using ANFIS and optimization with fuzzy modeling approach. *Energy and Buildings* **41**, 814–822.

Tahmasebi, P. & Hezarkhani, A. 2010. Application of adaptive neuro-fuzzy inference system for grade estimation; case study, Sarcheshmeh porphyry copper deposit, Kerman, Iran. *Australian Journal of Basic and Applied Sciences* **4**, 408–420.

Tahmasebi, P. & Hezarkhani, A. 2012. A hybrid neural networks-fuzzy logic-genetic algorithm for grade estimation. *Computers and Geosciences* **42**, 18–27.

Tütmez, B. 2005. *Reserve Estimation Using Fuzzy Set Theory*. PhD Thesis, Hacettepe University, Ankara–Turkey [unpublished].

Tütmez, B. 2007. An uncertainty oriented fuzzy methodology for grade estimation. *Computers and Geosciences* **33**, 280–288.

Tütmez, B., Tercan, A.E. & Kaymak, U. 2007. Fuzzy modeling for reserve estimation based on spatial variability. *Mathematical Geology* **39**, 87–111.

Tütmez, B. & Dağ, A. 2005. Use of fuzzy logic in lignite reserve estimation. *Energy Sources (Part B: Economics, Planning and Policy)* **2**, 93–103.

Zedef, V., Aslan, M., Kurt, H. & Şen, O. 1995. The genesis and geological-geochemical properties of Ağılönü (Beyşehir) barite occurrences. *Yerbilimleri-Geosound* **27**, 171–179.

Zhang, X.Q., Wang, H.B. & Yu, H.Z. 2007. Neural network based algorithm and simulation of information fusion in the coal mine. *Journal of the China University of Mining and Technology* **17**, 595–598.

Zhihong, L. & Zhizeng, L. 2008. Hand motion pattern classifier based on EMG using wavelet packet transform and LVQ neural networks. *In: IEEE International Symposium on IT in Medicine and Education*, 28–32.

Zimmerman, R.A. 1969. Stratabound barite deposits in Nevada. *Mineralium Deposita* **4**, 401–409.